

Short-channel effect and single-electron transport in individual indium oxide nanowires

Minkyung Jung¹, Hyoyoung Lee¹, Sunkyung Moon², Woon Song²,
Nam Kim², Jinhee Kim², Gunho Jo³ and Takhee Lee³

¹ National Creative Research Initiative, Center for Smart Molecular Memory, Electronics and Telecommunication Research Institute, Daejeon 305-700, Korea

² Korea Research Institute of Standard and Science, Daejeon 305-600, Korea

³ Department of Materials Science and Engineering, Gwangju Institute of Science and Technology, Gwangju 500-712, Korea

E-mail: hyoyoung@etri.re.kr

Received 30 August 2007

Published 4 October 2007

Online at stacks.iop.org/Nano/18/435403

Abstract

We have investigated the electric transport properties of individual In₂O₃ nanowire devices. We have found that the gate modulation characteristics depend strongly on the channel length. If the channel length is greater than 450 nm, the gate modulation curve exhibited field-effect transistor behavior with dominant n-channel current at room temperature. With the decrease of the channel length, the leakage current is increased due to the short-channel effect. For such short-channel devices, the gate modulation curve exhibited quasi-periodic current oscillations at low temperature, which are attributed to the Coulomb blockade of single-electron tunneling. Some devices showed two-fold periodicity in the Coulomb diamonds which may arise from the spin degeneracy of the single-particle energy levels.

1. Introduction

Due to their unique electrical and optical properties, semiconducting nanowires have drawn considerable attention recently. A variety of nanowire-based electronic devices have been realized. Among them are field-effect transistors (FETs), elementary logic circuits, resonant tunneling diodes, light-emitting diodes, nanolasers, and biochemical sensors [1–4]. Compared with their bulk counterparts, nanowires demonstrate additional functionality and/or superior performance, which were in part attributed to the quantum-confinement effect resulting from the low dimensionality of nanowires. Regarding the quantum confinement effect in nanowires, many experimental observations have been reported so far [5–12].

Compared with other semiconducting nanowires, chemically synthesized In₂O₃ nanowires are one of the less studied systems. This is rather surprising, considering that amorphous In/InOx film is one of the most studied disordered metal systems [13, 14]. Many interesting phenomena, including the superconductor–insulator transition, universal conductance

fluctuation, and Coulomb blockade of single-electron tunneling, were observed in amorphous In/InOx films [13, 14]. Most of these observations are focused on the effect of disorder in the electron transport in amorphous metal films. Recently, single-crystalline In₂O₃ nanowires have been synthesized by several groups. Compared with the amorphous film, single-crystalline In₂O₃ nanowires are expected to have fewer defects and the electron transport would be more ballistic. The effect of reduced dimensionality on the electron transport would be more pronounced in such single-crystalline nanowires than in amorphous film. But only a few studies have been reported so far on the electric transport properties of In₂O₃ nanowires [4, 15–18] and most of them [4, 15–17], with one exception [18], are focused on the sensor application of In₂O₃ nanowires. To understand how the reduced dimensionality changes the electric transport properties of In₂O₃ nanowires, an extensive study is yet to be performed.

In this paper, we present our study on the electric transport properties of individual In₂O₃ nanowire devices. We have found that the gate modulation characteristic depends strongly

Table 1. Summary of parameters for the different devices measured.

Device #	D (nm)	L (nm)	$R_{300\text{ K}}$ (k Ω)	$R_{2\text{ K}}$ (M Ω)
A	30	1500	—	—
B	30	450	—	—
C	30	180	320	6
D	30	200	148	2
E	60	300	80	1

on the channel length. If the channel length is greater than 450 nm, the gate modulation curve exhibited n-type FET behavior as reported in previous studies [15, 17]. With the decrease of the channel length, the threshold voltage shifted to negative voltages and even disappeared if the channel length became shorter than 180 nm. For most of the devices with a channel length shorter than 300 nm, the gate modulation curve exhibited quasi-periodic current oscillations at 2 K, attributed to the Coulomb blockade of single-electron tunneling. Some devices showed two-fold periodicity in the Coulomb diamonds, which may arise from the spin degeneracy of the single-particle energy levels.

2. Experimental details

The In_2O_3 nanowires used in the present study were grown by carbothermal reduction followed by the catalyst-mediated heteroepitaxial growth technique [19, 20]. At first, a 4:1 mixture (weight ratio) of In_2O_3 powder (99.995%) and graphite powder (99%) was placed in a quartz boat inside a tube reactor. Then, In_2O_3 nanowires were grown on a Si/SiO₂ substrate covered with 2 nm thick gold film used as a catalyst. During the growth, the temperature was set at 900–1000 °C, while Ar mixed with 5% O₂ was flowing at a rate of 50–100 sccm for ~35 min. Grown nanowires had diameters of 20–150 nm and lengths 2–10 μm . After the growth, the nanowires were dispersed in isopropanol solution. In order to fabricate a device, a droplet of the solution containing nanowires was deposited on an n⁺-Si substrate with a 300 nm-thick SiO₂ top layer. Patterns for metal electrodes were defined by standard electron-beam lithography. Since residual resist around the nanowires increases the contact resistance, samples were treated with an oxygen plasma. The oxygen plasma processing was carried out in 30 mTorr vacuum with an rf power of 50 W for 6 s. The metal electrodes were formed directly on In_2O_3 nanowires by successively depositing 10 nm thick Ti and 100 nm thick Au layers. After the metal deposition, no post-annealing was employed. The inset of figure 1 shows a scanning electron microscope (SEM) image of typical fabricated devices. As seen in the figure, metal electrodes of width 200 nm are separated by 0.18–1.5 μm . A total of five samples was fabricated and studied. The sample parameters are shown in table 1.

3. Results and discussion

First, we have studied the channel length dependence of the gate modulation characteristics. We have measured the gate modulation (I - V_G) curves of a single nanowire with varying inter-electrode distances. The inset of figure 1 shows the SEM image of the devices. The nanowire has a diameter

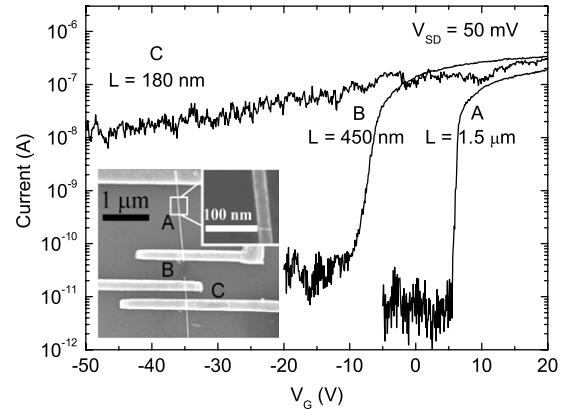


Figure 1. The gate modulation curves of the In_2O_3 nanowire devices with different channel lengths. Measurement was done at room temperature. Devices A, B, and C, whose electrodes are attached to the same nanowire, have channel lengths of 1.5, 0.45, and 0.18 μm , respectively. The inset shows a scanning electron microscope image of typical devices. Device B was broken after repeated measurements.

of about 30 nm and the inter-electrode distances were 1.5, 0.45, and 0.18 μm for the devices A, B, and C, respectively. Figure 1 shows the gate modulation curves of each device measured at 300 K with source–drain bias voltage of $V_{\text{SD}} = 50$ mV. For device A, with the longest channel length, the gate modulation curve exhibits clear n-channel dominant FET behavior with the threshold voltage of 6.2 V. Previous studies also reported dominant n-channel current in In_2O_3 nanowires, due to the O₂ vacancies [15]. We have estimated the mobility of device A. The gate capacitance is estimated to be $C_G \sim 87.9$ aF, by using the relation $C_G \approx 2\pi\epsilon\epsilon_0L/\ln(4h/d)$, where h , d , and ϵ are the oxide thickness, nanowire diameter, and dielectric constant of SiO₂ film, respectively [21]. The trans-conductance, $g_m = dI/dV_G$ at $V_{\text{SD}} = 50$ mV, was obtained to be $\sim 5.7 \times 10^{-8}$ A V⁻¹. From $dI/dV_G = g_m = \mu(C_G/L^2)V_{\text{SD}}$, the electron mobility was estimated to be $\mu \sim 290$ cm² V⁻¹ s⁻¹ [22]. Note that such high mobility exceeds the highest reported value in In_2O_3 nanowire FETs [15, 17].

As the channel length decreased to 450 nm, the threshold voltage shifted negatively to -6.7 V and the trans-conductance (dI/dV_G) at the n-channel threshold voltage was reduced greatly. For device C with the shortest channel length, the n-channel threshold voltage could not be identified in the measured voltage range and the on-current showed only a small change up to gate voltage $V_G = -50$ V. Such deterioration of the FET behavior with the decrease of the channel length was also observed in a conventional semiconducting device with the channel length too short to be depleted by gate bias voltage [22]. Our observations indicate that such a short channel effect occurs in In_2O_3 nanowires with the channel length smaller than ~ 0.3 μm .

We have also measured the electric transport properties of short-channel devices (channel length ≤ 300 nm) at low temperatures. As the temperature was decreased from 300 to 2 K, the sample resistance increased from a few hundred k Ω up to a few M Ω . Figure 2(a) shows the temperature-dependent gate modulation curves of another sample (D) with source–drain bias voltage of $V_{\text{SD}} = 500$ μV . The diameter and channel

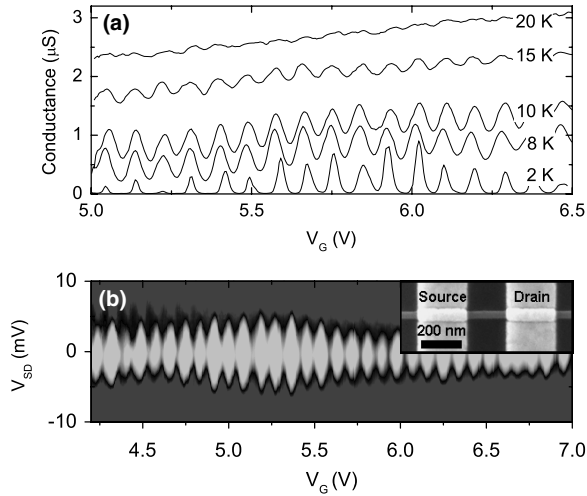


Figure 2. (a) The temperature-dependent gate modulation curves of device D. The nanowire diameter and channel length were 30 nm and 200 nm, respectively. The source–drain bias was $V_{SD} = 500 \mu\text{V}$. (b) Two-dimensional plot of the differential conductance, dI/dV_{SD} , as a function of the source–drain voltage, V_{SD} , and the gate voltage, V_G . Dark areas correspond to high values of dI/dV_{SD} . The inset shows the SEM image of the fabricated device.

length of the nanowire were 30 nm and 200 nm, respectively. At low temperatures, the gate modulation curve exhibited quasi-periodic current oscillations. The current peaks are well separated by the conductance gap. Repeated measurements give almost identical results and no hysteresis was observed. Such quasi-periodic current oscillation, known as the Coulomb oscillation, is attributed to the Coulomb blockade of single-electron tunneling [25]. The Coulomb oscillation becomes more evident with the decrease of temperature and persists

up to 15 K before it is thermally smeared out, as shown in figure 2(a). Each peak in a Coulomb oscillation corresponds to the number of electrons in a quantum dot (QD) [6, 9]. We could identify more than 100 peaks but complete depletion of electrons was not observed.

Figure 2(b) shows the differential conductance, dI/dV_{SD} , as a function of V_{SD} and V_G . Diamond-like patterns, so-called Coulomb diamonds, are apparent. By sweeping V_G along with $V_{SD} \approx 0$, N changes one by one where neighboring Coulomb diamonds contact each other. Note that each Coulomb diamond has relatively well-defined edges and a resonance point, suggesting that device D has single QD inside it [6, 7]. From the height of the Coulomb diamond, we can estimate the addition energy, the energy required to add one extra electron into the QD, $E_{\text{add}} \approx 3\text{--}5 \text{ meV}$. The addition energy E_{add} is defined by $E_{\text{add}} = E(N+1) - E(N)$, where $E(N)$ is the total energy required to add N electrons into the QD. In general, E_{add} is the sum of the charging energy $E_C = e^2/C_\Sigma$ and the energy level spacing Δ [25, 26].

We have measured the electric transport properties of another device (E). For device E, as shown in figure 3(b), the diameter and channel length are 60 nm and 300 nm respectively. Figure 3(a) shows the gate modulation of device E at the temperature of 2 K with source–drain bias voltage of $V_{SD} = 500 \mu\text{V}$. Though not evident, the gate modulation curve seemed to show repeated pairs of current peaks, suggesting a two-fold periodicity in the Coulomb oscillation. Such two-fold periodicity becomes clearer in the Coulomb diamond diagram shown in figure 3(c). As seen in the figure, a larger diamond is neighbored by a smaller one. The larger the Coulomb diamond is, the greater the addition energy is. So, our observation implies that the addition energy is oscillating with two-fold periodicity. Such two-fold periodicity in the Coulomb diamond is reminiscent of the two-fold shell filling in a symmetric QD. For a symmetric QD with degenerated single-particle energy

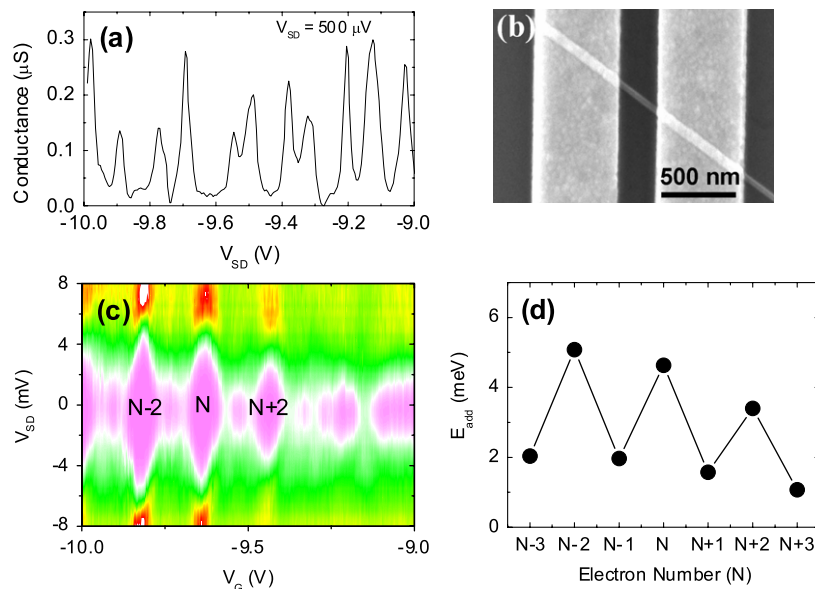


Figure 3. (a) The gate modulation curves of device E measured at 2 K with $V_{SD} = 500 \mu\text{V}$. (b) The SEM image of device E. The nanowire diameter and channel length are 60 nm and 300 nm, respectively. (c) The two-dimensional plot of the differential conductance as a function of the source–drain voltage, V_{SD} , and the gate voltage, V_G , for device E shows clear two-fold degeneracy. (d) The addition energy as a function of electron number, N , shows two-fold periodicity.

levels, the addition energy would show shell-filling structure in the Coulomb diamond. The periodicity depends on the number of the degenerated states. Both two- and four-fold shell filling were observed in a single-wall carbon nanotube [23, 24]. In general, two-fold shell filling is observed more frequently and is in many cases attributed to the spin degeneracy of the single-particle energy levels. Inside the In_2O_3 nanowire there would be many defects and/or disorder which could break the angular momentum symmetry of the QD. The spin degeneracy, on the other hand, would be robust and thus could be preserved for such a device. So, we assume that the QD has two-fold degenerated single-particle energy levels arising from the spin angular momentum symmetry. For such a system, the addition energy $E_{\text{add}}(N)$ becomes $E_C + \Delta$ for even N and E_C for odd N . From figure 3(c), we could estimate the charging energy $E_C = 1\text{--}2$ meV and the energy level spacing $\Delta = 2\text{--}3$ meV, and this is plotted in figure 3(d) [25, 26]. Such even-odd shell filling could be observed if the charging energy is comparable to the energy level spacing. For device D, no even-odd shell filling was observed. This can be explained if time-reversal symmetry is broken for some reason, or the charging energy is much greater than the energy level spacing. The latter would be more likely, since no magnetic elements are added to the nanowire during synthesis. We, however, cannot provide a satisfactory explanation for the occurrence and absence of the even-odd shell filling in In_2O_3 nanowires.

4. Conclusion

In summary, we have investigated the electron transport properties of individual In_2O_3 nanowire devices. For long channel devices, n-type field-effect transistor characteristics were apparent at room temperature. For devices with the channel length shorter than 300 nm, clear Coulomb blockade oscillations were observed at low temperature. The two-fold periodicity in the Coulomb diamonds, which we attributed to the spin degeneracy of the single-particle energy level, is the first observation of energy level degeneracy in In_2O_3 nanowire devices. We believe that our result can be helpful to develop future electronic devices based on nanowires.

Acknowledgments

MJ thanks Professor K Hirakawa for useful discussions. This work was supported by the Creative Research Initiatives Program research fund (Project title: Smart Molecular Memory) of MOST/KOSEF.

References

- [1] Lieber C M 2003 *Mater. Res. Bull.* **28** 486
- [2] Thelander C *et al* 2006 *Mater. Today* **9** 28
- [3] Samuelson L *et al* 2004 *Physica E* **25** 313
- [4] Rout C S, Ganesh K, Govindaraj A and Rao C N R 2006 *Appl. Phys. A* **85** 241
- [5] Thelander C, Martensson T, Bjork M T, Ohlsson B J, Larsson M W, Wallenberg L R and Samuelson L 2003 *Appl. Phys. Lett.* **83** 2052
- [6] De Franceschi S, Van Dam J A, Bakkers E P A M, Feiner F, Gurevich L and Kouwenhoven L P 2003 *Appl. Phys. Lett.* **83** 344
- [7] Bjork M K, Thelander C, Hansen A E, Jensen L E, Larsson M W, Wallenberg L R and Samuelson L 2004 *Nano Lett.* **4** 1621
- [8] Bjork M T, Fuhrer A, Hansen A E, Larsson M W, Froberg L E and Samuelson L 2005 *Phys. Rev. B* **72** 201307
- [9] Zhong Z, Fang Y, Lu W and Lieber C M 2005 *Nano Lett.* **5** 1143
- [10] Doh Y J, van Dam J A, Roest A L, Bakkers E P A M, Kouwenhoven L P and De Franceschi S 2005 *Science* **309** 272
- [11] van Dam J A, Nazarov Y V, Bakkers E P A M, De Franceschi S and Kouwenhoven L P 2006 *Nature* **442** 667
- [12] Pfund A, Shorubalko I, Leturcq R and Ensslin K 2006 *Appl. Phys. Lett.* **89** 252106
- [13] Chandrasekhar V, Ovadyahu Z and Webb R A 1991 *Phys. Rev. Lett.* **67** 2862 and reference therein
- [14] Chandrasekhar V and Webb R A 1994 *J. Low Temp. Phys.* **97** 9 and reference therein
- [15] Zhang D, Li C, Han S, Liu X, Tang T, Jin W and Zhou C 2003 *Appl. Phys. Lett.* **82** 112
- [16] Li C, Zhang D, Liu X, Han S, Tang T, Han J and Zhou C 2003 *Appl. Phys. Lett.* **82** 1613
- [17] Lei B, Li C, Zhang D, Tang T and Zhou C 2004 *Appl. Phys. A* **79** 439
- [18] Liu F, Bao M, Wang K L, Li C and Zhou C 2005 *Appl. Phys. Lett.* **86** 213101
- [19] Ng H T, Chen B, Li J, Han J, Meyyappan M, Wu J, Li S X and Haller E E 2003 *Appl. Phys. Lett.* **82** 2023
- [20] Kam K C, Deepak F L, Cheetham A K and Rao C N R 2004 *Chem. Phys. Lett.* **397** 329
- [21] Martel R, Schmidt T, Shea H R, Hertel T and Avouris Ph 1998 *Appl. Phys. Lett.* **73** 2447
- [22] Taur Y and Ning T H 1998 *Fundamentals of Modern VLSI Devices* (Cambridge: Cambridge University Press)
- [23] Cobden D H and Nygard J 2002 *Phys. Rev. Lett.* **89** 046803
- [24] Liang W, Bockrath M and Park H 2002 *Phys. Rev. Lett.* **88** 126801
- [25] Grabert H and Devoret M H (ed) 1992 *Single Charge Tunneling: Coulomb Blockade Phenomena in Nanostructures (Nato Science Series B)* (New York: Plenum)
- [26] Sohn L L, Kouwenhoven L P and Schon G (ed) 1997 *Mesoscopic Electron Transport (Nato Science Series E)* (Dordrecht: Kluwer) pp 105–214